# Estimation of Losses in the (RE)BCO Two-Coil Insert of the NHMFL 32 T All-Superconducting Magnet

E. Berrospe-Juarez, V. M. R. Zermeño, F. Trillaud, A.V. Gavrilin, F. Grilli, D. V. Abraimov, D. K. Hilton, and H. W. Weijers

***Abstract*—(RE)BCO commercial coated superconductors have been gaining an increasing interest due to the potentialities of using them in high-field magnets. The leading project is the 32 T user magnet recently tested successfully at full field at the National High Magnetic Field Laboratory (NHMFL), Tallahasee, FL, USA. This state-of-the-art high-field all-superconducting magnet, bath-cooled at 4.2 K, is comprised of a two-nested-coil insert pancake-wound with (RE)BCO tapes supplied by SuperPower Inc. and a multi-coil low temperature superconductors (LTS) outsert. To ensure the magnet's reliable operation, it is important to estimate the hysteresis losses. Such an estimate will allow implementing safe operational procedures to avoid premature quenching and, in the worst case scenario, insert failure. The insert coils have thousands of turns with notable variations in the critical current. Therefore, estimating the losses in such a large superconducting magnet presents a significant challenge. We propose here a new approach relying on a multiscale scheme to achieve a high computational efficiency. This new method is flexible enough to simulate different sections of the entire insert with the right level of detail while providing a larger computational speed than other approaches using the finite element method. Estimates of the hysteresis losses in the insert coils for a ramping operation sequence are presented.**

***Index Terms*—AC losses, HTS magnets, (RE)BCO coils, finite element methods.**

## I. Introduction

THREE decades after the discovery of the high temperature superconductors (HTS), the commercial (RE)BCO tapes have matured to the point that they can provide performances for high magnetic field applications. In particular, their high strength and remarkably high critical current are the key enablers to generate very high continuous magnetic fields that cannot be achieved with low temperature superconductors (LTS).

A new generation of high magnetic field user magnets is being developed at the National High Magnetic Field Laboratory (NHMFL) in an effort to increase its capability of providing magnetic fields above 30 T. The first magnet in the series is a 32-T all-superconducting one, which consists of a 15 T multi-coil LTS outsert custom-made by Oxford Instruments, Inc. and an innovative 17 T (RE)BCO-tape wound dual-coil insert operated at 4.2 K [1], [2]. The (RE)BCO tapes were supplied by SuperPower, Inc. It is the first magnet utilizing two (RE)BCO coils having thousands of turns. Besides minimizing the helium consumption, it is important to ensure the safe operation of the magnet during the changes in magnetic field required by the users. Thus, the risks associated with the technology should be clearly assessed. Any changes of magnetic field generated by the background LTS outsert and/or the HTS insert are expected to result in dissipations of stored energy absorbed by the cryogenic system.

Part of this assessment, a preliminary model was developed to quantify the losses in prototype coils of a few pancakes [3]. This model is based on the homogenization technique [4]. In the present work, a different, advanced approach is proposed to assess the hysteresis losses in the actual two-coil insert. The simulation that we performed enables us to estimate the self-field losses in the insert when the transport current in it is a triangle-shaped ramp cycle 2 min long, which does not represent the generic operation of the magnet [1], but represents an interesting "limiting case" in terms of hysteresis losses. The proposed approach is based on the iterative multi-scale method put forward in [5]. This method allows analyzing such a large system with a lesser computational load and shorter computation time and provides an easy handling of the variations in the critical current of the batches of (RE)BCO tapes in the insert.

Section II contains a brief description of the iterative multi-scale method and the interpolation procedure to estimate the current density in the tapes that are not explicitly analyzed. The description of the HTS insert and its layout is presented in Section III. The results of the simulations, carried out with COMSOL Multiphysics 5.3, are presented in Section IV.

## II. Iterative Multi-Scale Method

The main drawback of the multi-scale method is found in the difficulty to estimate accurately the background magnetic field

Manuscript received August 27, 2017; accepted January 1, 2018. Date of publication January 9, 2018; date of current version January 26, 2018. This work was supported in part by the Programa de Maestría y Doctorado en Ingeniería of the Universidad National Autónoma de México (UNAM) and the Consejo Nacional de Ciencia y Tecnología (CONACYT) under CVU: 490544, and in part by the DGAPA-UNAM under Grant PAPIIT-2017 #TA100617. *(Corresponding authors: E. Berrospe-Juarez; V. M. R. Zermeño; F. Trillaud.)*

E. Berrospe-Juarez is with the Posgrado en Ingeniería Eléctrica, Universidad Nacional Autónoma de México, Mexico City 04510, México (e-mail: eberrospej@iingen.unam.mx).

V. M. R. Zermeño was with the Karlsruhe Institute of Technology, Karlsruhe 76131, Germany (e-mail: victor.zermeno@kit.edu).

F. Trillaud is with the Instituto de Ingeniería, Universidad Nacional Autónoma de México, Mexico City 04510, México (e-mail: ftrillaudp@iingen.unam.mx).

A. V. Gavrilin, D. V. Abraimov, D. K. Hilton, and H. W. Weijers are with the National High Magnetic Field Laboratory, Tallahasee, FL 32310 USA.

F. Grilli is with the Karlsruhe Institute of Technology, Karlsruhe 76131, Germany (e-mail: francesco.grilli@kit.edu).

Color versions of one or more of the figures in this paper are available online at http://ieeexplore.ieee.org.

Digital Object Identifier 10.1109/TASC.2018.2791545

produced by an entire magnet [6], [7]. A solution enabling one to overcome this limitation is the iterative multi-scale method, whose accuracy has been verified in [5] by comparing the results obtained with the use of the multi-scale models, for a smaller system, with those by the corresponding *H*-formulation model.

The approach is built upon two submodels and based on solving Maxwell's equations in 2D, using Finite Element Method (FEM). The first submodel, here called "insert submodel," is that of the entire insert and solves a magneto-static problem using an **A**-formulation of Maxwell's equations. The insert including all its tapes is modelled to compute the distribution of the magnetic field throughout it. Subsequently, the second "single-tape submodel" simulates several tapes in significant positions ("analyzed tapes"), using the *H*-formulation [8]. The magnetic field corresponding to the boundary of each analyzed tape computed from the insert submodel is exported to the single-tape submodel as a time-varying Dirichlet boundary condition. The current density distribution in the remaining "non-analyzed tapes" is interpolated. Then, the new current density distribution in the entire insert is exported to the insert submodel and a new distribution of the magnetic field is computed. Similarly, the hysteresis losses are calculated in the analyzed tapes and the result is used to approximate the losses in the non-analyzed tapes. The process begins with a uniform current density in all the tapes, and it is repeated until the convergence criterion is met. In this work, the criterion $\varepsilon$ is tested on the relative error of the total losses $Q$ from one iteration to the next, as follows

$$\varepsilon > \frac{|Q_n - Q_{n-1}|}{Q_n}, \tag{1}$$

where the subscript $n$ indicates the iteration number.

Within every pancake, the current density of the analyzed tapes is used to approximate the current density in the non-analyzed tapes. If one uses linear interpolation, then non-physical current density distributions are obtained. A new technique is used in this work, which has proven to give satisfactory results [5]. This new interpolation technique is based on the Inverse Cumulative Distribution Function (ICDF) presented in [9].

TABLE I
PARAMETERS OF INSERT COILS

| Parameter | Coil 1 | Coil 2 |
|---|---|---|
| Inner radius | 20 mm | 82 mm |
| Outer radius | 70 mm | 116 mm |
| Height | 178 mm | 320.4 mm |
| Pancakes | 40 | 72 |
| Turns/Pancake | 253 | 145 |
| (RE)BCO layer width | 4 mm | 4 mm |
| (RE)BCO layer thickness | 1 $\mu$m | 1 $\mu$m |
| Single-tape model width | 4.45 mm | 4.45 mm |
| Single-tape model thickness | 197.63 $\mu$m | 234.48 $\mu$m |

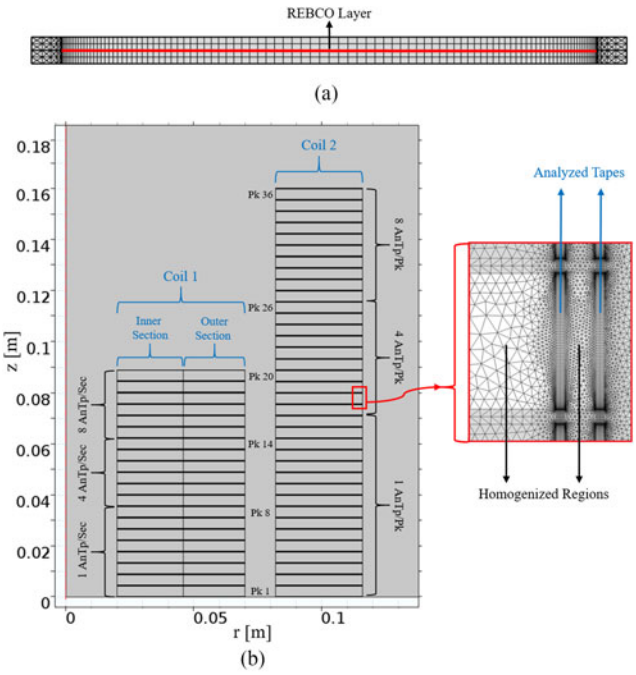


Fig. 1. (a) Mesh of the single-tape submodel. (b) The insert submodel. Each pancake of Coil 1 has two sections. The zoomed fragment shows the local mesh in the outer part of pancake 18 of Coil 2. The mesh of both the analyzed tapes and the homogenized regions are shown. The notation "AnTp/Pk" stands for Analyzed Tapes per Pancake.

## III. INSERT AND ITS MODELLING

A detailed description of the 32 T magnet can be found in [1], [2]. The present work focuses solely on the 17 T HTS insert. It is composed of two nested coils assembled from double pancakes/modules co-wound with sol-gel plated stainless steel strips and (RE)BCO tapes. The sol-gel plated stainless steel strips increase the mechanical strength of the winding to handle the extreme Lorentz's forces.

### A. Insert Description

The (RE)BCO tapes are 4 mm wide and have a thickness in the range of 0.16 to 0.18 mm. Despite the thickness variations, for simplicity, it is assumed that the pancakes inside the same coil have the same number of turns. Table I summarizes the insert salient parameters. Our model of a tape, shown in Fig. 1(a), includes a single 1 $\mu$m thick layer of (RE)BCO surrounded by a non-electric and non-magnetic region, which lumps the stabilizer, substrate and other layers of the tape, and the stainless-steel strip as well. The (RE)BCO layer is properly meshed with rectangular elements: 1 across its thickness and 100 along the width. The mesh is graded with increasing number of elements at the extremities. Fig. 1(b) shows the axisymmetric insert submodel. It should be noted that the real insert does not present symmetry, because of the variation of the critical current in the different tape batches.

The geometry of the insert submodel has been further simplified to lower the computational burden. The simplification consists in homogenizing the non-analyzed tapes while keeping the single-tape submodel geometry for the analyzed tapes. The interpolated current density that is imposed in the homogenized regions is multiplied by the ratio of the (RE)BCO layer thickness to the single-tape submodel thickness. In those regions, the mesh is triangular with a refined mesh close to the analyzed

tapes and a coarse mesh within the rest. The variation in the critical current from batch to batch forces each pancake of Coil 1 to be divided in two sections, each section having its own critical current. As shown in [4], [7], there exist more significant variations in the losses and current density distribution in the tapes located at the inner and outer layers of the top and bottom pancakes. Therefore, a greater number of analyzed tapes should be provided at those locations. Also, the results presented in [7] indicate that the lower pancakes have the lower losses, and the losses exhibit significant increments from one pancake to another. Hence, in order to reduce the computation time without compromising the accuracy of the results the lower pancakes of Coil 2 have one analyzed tape per pancake, the same as each section of the lower pancakes of Coil 1 does. The number of analyzed tapes per pancake or pancake's section increases to four and ends in eight in the upper pancakes. In this manner, the number of analyzed tapes in each pancake is increased in the upper pancakes where larger losses are expected.

### *B. Critical Current Density Model*

Using the critical current measurements done by the NHMFL at 4.2 K for different orientations of the magnetic field, the critical current density $J_c$ was reconstructed following the method proposed in [10] and was fitted to the following relation,

$$J_c\left(B_r, B_z\right) = \frac{\beta \cdot J_{c0}}{\left(1 + \frac{\sqrt{k^2 B_z^2 + B_r^2}}{B_0}\right)^{\alpha}}, \tag{2}$$

where $B_r$ and $B_z$ are the radial and axial components of the magnetic field, respectively. The fitting parameters are $J_{c0} = 2.896 \cdot 10^{12}$ [A $\cdot$ m$^{-2}$], $B_0 = 0.4674$ T, $k = 9.13 \cdot 10^{-3}$, $\alpha = 0.7518$. The value of coefficient $\beta$, estimated experimentally by the NHMFL, is oscillating between 0.63 and 1.5, $\beta$ provides the magnitude of variation of critical current around the reference value $J_{c0}$ from batch to batch. Thus, it takes a different value for each pancake of Coil 2 and for each section of each pancake of Coil 1.

### *C. Estimation of Losses*

The resistivity of the superconducting layer is modeled as,

$$\rho_{HTS} = \frac{E_c}{J_c(B)} \left| \frac{J}{J_c(B)} \right|^{n-1}, \tag{3}$$

with $n = 25$ and $E_c = 1\,\mu$V$\cdot$cm$^{-1}$.

The local losses in a given analyzed tape are given by

$$Q_{p,t} = \int_T dt \int_\Omega 2\pi r E \cdot J d\Omega, \tag{4}$$

where $T$ is the analyzed lapse as shown in Fig. 2, and $\Omega$ is the cross section of the tape.

In the non-analyzed tapes of the pancakes or sections of pancakes where only one analyzed tape is, the losses are considered to be equal to those of the analyzed tapes. The losses in the non-analyzed tapes in the rest of the pancakes are found by spline interpolation. Finally, the global losses are computed by summing the losses of all the tapes and multiplying by 2 because of the symmetry around the *r* axis (see Fig. 1).

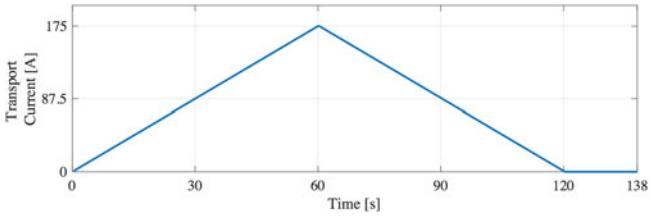


Fig. 2. Analyzed ramp cycle of duration equal to 120 s, followed by 18 s at 0 A ($T = 138$ s).

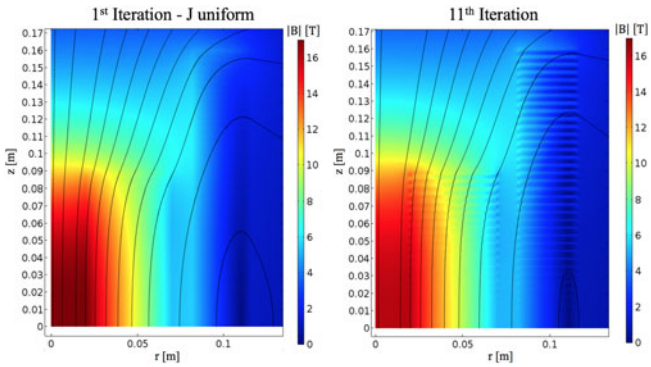


Fig. 3. Magnetic field magnitude at 60 s, the peak of the ramping cycle.

## IV. Results and Discussion

The self-field hysteresis losses of the insert during a ramping cycle are evaluated. The insert is assumed to be charged linearly from 0 A to 175 A during 1 min and subsequently discharged at the same rate. The ramping up and down combined lasts 120 s and additionally 18 s are simulated to analyze the losses in the first instants of the relaxation process once the transport current in the insert is set back to zero (see Fig. 2). The iterative multi-scale method was used with a convergence criterion of $\varepsilon = 1 \cdot 10^{-3}$. Fig. 3 shows the magnetic field magnitude for the 1st iteration, where the current density is uniform, and for the 11th iteration, when the convergence criterion is met. The current density distribution for six selected pancakes in each coil is shown in Fig. 4, where one can see that the non-uniformity of the critical current makes a difference in the current density distribution for different sections of Coil 1.

Fig. 5 presents the losses for the same pancakes shown in Fig. 4. The *x*-axis represents the number of tapes in the pancakes. The losses are incremented due to the shielding effect in the inner and outer tapes of each coil. The zoomed part in Fig. 5 is placed in the transition from the inner to the outer section of Coil 1. This zoom shows that the iterative multi-scale method has enough resolution to reproduce the losses variations produced not only due to variations in the background field, but also due to variations in $J_c$. The coefficient $\beta$ in (4) takes values between 1.5 and 1.4, for the inner and outer sections of each pancake, respectively; this change in $\beta$ results in the increment in the local losses of the last tape of inner section. For pancake 17 of

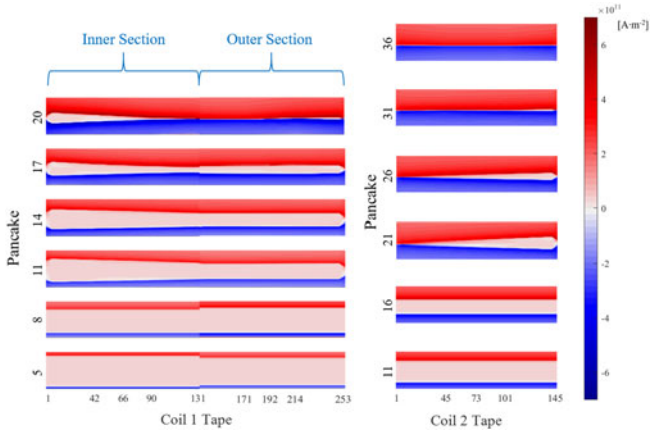


Fig. 4. Current density distribution within the selected pancakes at 60 s, the peak of the ramping cycle.

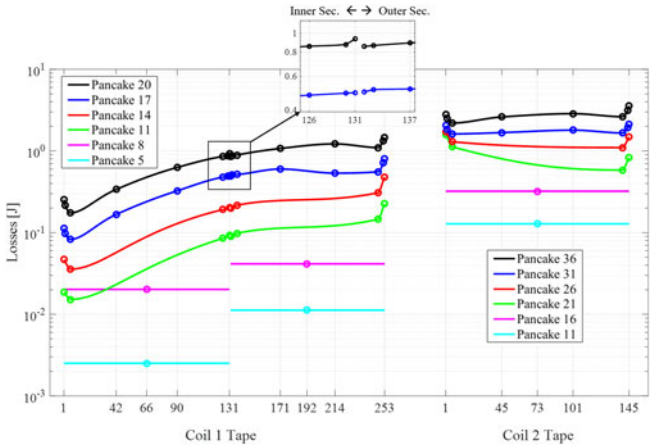


Fig. 5. Losses in selected pancakes. The zoom is placed in the transition from inner section to outer section of the pancakes 20 and 17 of Coil 1.

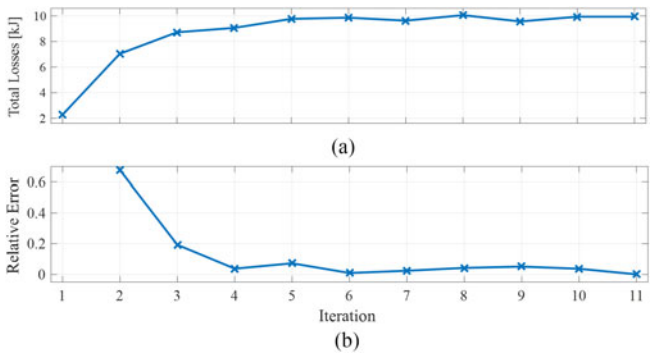


Fig. 6. (a) Total losses in the insert during the ramping cycle (the outsert is off). (b) Relative error.

Coil 1, the $\beta$-value goes from 1.08 to 1.09, and this variation does not produce a significant change in the local losses.

The total losses in the insert and the relative error are shown in Fig. 6. The total losses at the 11th iteration are $Q_{11} = 9.946$ kJ, and the relative error, at the same iteration equals $7 \cdot 10^{-4}$ that is lower than the criterion, $\varepsilon = 1 \cdot 10^{-3}$. Also, it is worth noting that the relative error is lower than $5.2 \cdot 10^{-2}$ for the iterations larger than 6. Another important result is that the losses in Coil 2 are clearly higher than the losses in Coil 1, and Coil 2 gives 82% of the total losses. This substantial difference in the losses is due to a larger number of pancakes in Coil 2 (72 pancakes) than the number of pancakes in Coil 1 (40 pancakes). Although the field is stronger in Coil 1, it is at a significantly larger angle ("more perpendicular") to the face of the tapes in the outer pancakes of Coil 2.

Back to Figs. 4 and 5, one can readily see that the shielding effect and its respective increment in the local losses are not reproduced when just one tape is analyzed in each pancake. Of course, this fact hinders the correct estimation of the local losses, but the impact on the total losses is minor. There are 24 pancakes (out of the grand total of 56) with one analyzed tape, 8 in Coil 1 and 16 in Coil 2, these pancakes give 4.8% of the total losses. The 8 pancakes with one analyzed tape in Coil 1 give 1.7% of the losses in Coil 1, while 16 pancakes with one analyzed tape in Coil 2 are responsible for the 5.4% of the losses in Coil 2. A similar analysis shows that the upper half of Coil 2 adds up to 75% of the total losses.

Although the single-tape submodel includes a restriction to impose the transport current, not to mention that the ICDF interpolation method guarantees preservation of the transport current, there exists a distortion in the total transport current density due to the coarse mesh in the bulk regions away from the analyzed tapes. However, the influence of such a distortion on the current density is markedly small.

A desktop computer (6 cores, Intel (R) Xeon(R) ES-2630, 2.2 GHz, 64 GB RAM) was used to conduct the simulations. The time required to run the insert submodel is around 1.5 hour. Every single tape simulation requires an average of 8 min. Since we have 296 analyzed tapes in total, each iteration of the iterative multi-scale method takes about 42 hours. It is important to keep in mind that the single tape analyses can be parallelized. This also shows the power and scalability of the multi-scale method, as the calculations can be performed by means of a commercially available desktop computer, which does not have the memory and computer power of a dedicated cluster supercomputer.

## V. Conclusion

The hysteresis losses in the actual pancake-wound (RE)BCO coils of the 32 T all-superconducting user magnet insert were analyzed in detail using a novel iterative multi-scale method. The pancakes of Coil 2 (the outer one) of the insert exhibit higher hysteresis losses than those of Coil 1 (the inner one). The losses in turns of the same pancakes of Coil 2 are quite similar, while in Coil 1, the closer a given turn to the outer diameter, the higher the losses in it. It is so because the background field is more perpendicular to the flat face of the tapes at the outer part of Coil 1 than in Coil 2.

The present work demonstrates that the iterative multi-scale method is suitable to analyze the entire 17 T multi-pancake insert using an ordinary desktop computer with reasonable computation times for any required accuracy. It should be noted that a better accuracy is achieved by simply increasing the number of

analyzed tapes at key locations. Additionally, it is shown that the proposed method provides better results than the classic multi-scale method. Indeed, the iterative approach leads to a better resolution on the background magnetic field, which yields a more accurate distribution of current density and subsequently a better estimation of the total losses. As a proof, the total losses at the last iteration of the iterative multi-scale method are more than four times larger than those obtained after the first iteration, corresponding to the classic multi-scale method.

## REFERENCES

[1] H. W. Weijers *et al.*, "Progress in the development and construction of a 32-T superconducting magnet," *IEEE Trans. Appl. Supercond.*, vol. 26, no. 4, Jun. 2016, Art. no. 4300807.

[2] W. D. Markiewicz *et al.*, "Design of a superconducting 32 T magnet with REBCO high field coils," *IEEE Trans. Appl. Supercond.*, vol. 22, no. 3, Jun. 2012, Art. no. 4300704.

[3] J. Xia, H. Bai, J. Lu, A. Gavrilin, Y. Zhou, and H. Weijers, "Electromagnetic modeling of REBCO high field coils by H-formulation," *Supercond. Sci. Technol.*, vol. 28, no. 12, p. 125004, Oct. 2015.

[4] V. Zermeno, A. Abrahamsen, N. Mijatovic, B. Jensen, and M. Sørensen, "Calculation of alternating current losses in stacks and coils made of second generation high temperature superconducting tapes for large scale applications," *J. Appl. Phys.*, vol. 114, no. 17, p. 173901, 2013.

[5] E. Berrospe-Juarez, V. Zermeno, F. Trillaud, and F. Grilli, "Iterative multi-scale method for estimating hysteresis losses in coils made of HTS conductors," 2017. [Online]. Available: https://arxiv.org/abs/1711.07447

[6] L. Quéval and H. Ohsaki, "AC Losses of a grid-connected superconducting wind turbine generator," *IEEE Trans. Appl. Supercond.*, vol. 23, no. 3, Jun. 2013, Art. no. 5201905.

[7] L. Quéval, V. M. R. Rodríguez-Zermeño, and F. Grilli, "Numerical models for ac loss calculation in large-scale applications of HTS coated conductors," *Supercond. Sci. Technol.*, vol. 29, no. 2, 2016, Art. no. 024007.

[8] R. Brambilla, F. Grilli, and L. Martini, "Development of an edge-element model for AC loss computation of high-temperature superconductors," *Supercond. Sci. Technol.*, vol. 20, no. 1, p. 16–24, 2006.

[9] A. Read, "Linear interpolation of histograms," *Nuclear Instruments Methods Phys. Res.*, vol. 425, no. 1–2, pp. 357–360, 1999.

[10] V. M. R. Rodríguez-Zermeño, K. Habelok, M. Stępień, and F. Grilli, "A parameter-free method to extract the superconductor's Jc(B, $\theta$) field-dependence from in-field current–voltage characteristics of high temperature superconductor tapes," *Supercond. Sci. Technol.*, vol. 30, no. 3, 2017, Art. no. 034001.